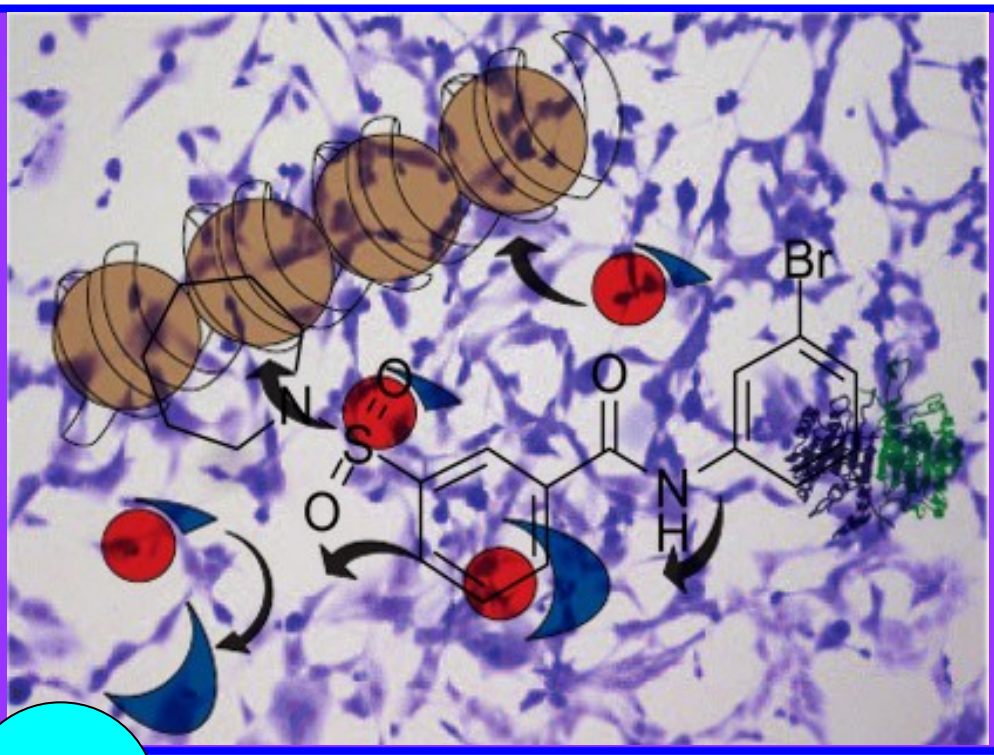

BJP

Bangladesh Journal of Pharmacology

Research Article

Inhibitory effect of AK-7 mediates by apoptosis, increases DNA fragmentation and caspase-3 activity in human glio-blastoma multiforme cells

A Journal of the Bangladesh Pharmacological Society (BDPS)
Journal homepage: www.banglajol.info; www.bdpsjournal.org
Abstracted/indexed in Academic Search Complete, Agroforestry Abstracts, Asia Journals Online, Bangladesh Journals Online, Biological Abstracts, BIOSIS Previews, CAB Abstracts, Current Abstracts, Directory of Open Access Journals, EMBASE/Excerpta Medica, Global Health, Google Scholar, HINARI (WHO), International Pharmaceutical Abstracts, Open J-gate, Science Citation Index Expanded, SCOPUS and Social Sciences Citation Index
Bangladesh J Pharmacol 2022; 17: 42-50
ISSN: 1991-0088

Inhibitory effect of AK-7 mediates by apoptosis, increases DNA fragmentation and caspase-3 activity in human glioblastoma multiforme cells

Ebru Güçlü, İlknur Çınar Ayan and Hasibe Vural

Department of Medical Biology, Meram Faculty of Medicine, Necmettin Erbakan University, Konya, Turkey.

Article Info

Received: 22 May 2022
Accepted: 5 June 2022
Available Online: 6 June 2022
DOI: 10.3329/bjp.v17i2.59809

Cite this article:
Güçlü E, Ayan IC, Vural H. Inhibitory effect of AK-7 mediates by apoptosis, increases DNA fragmentation and caspase-3 activity in human glioblastoma multiforme cells. Bangladesh J Pharmacol. 2022; 17: 42-50.

Abstract

Sirtuins (SIRTs) which are nicotinamide adenine dinucleotide (NAD+) dependent class III histondeacetylases have a controversial role in cancer. In this study, the effect of pharmacological inhibition of AK-7, a SIRT2 inhibitor, was investigated in U87 glioblastoma multiforme cells. The cytotoxic effect of AK-7 was evaluated by XTT analysis. After AK-7 treatment, colony forming capacity of cells was determined and apoptosis was evaluated. The expression levels of apoptosis-related genes were determined by qRT-PCR. According to the results, AK-7 inhibited cell proliferation in a dose- and time-dependent manner. After AK-7 treatment, the colony forming capacity of U87 cells was suppressed. And, AK-7 increased apoptosis rate, DNA fragmentation, and caspase-3 activity. According to qRT-PCR, a significant increase was observed in expression levels of apoptosis-related genes. This study revealed that AK-7 inhibits cell proliferation and induces apoptosis in glioblastoma multiforme cells and SIRT2 inhibition can be evaluated as a therapeutic approach in glioblastoma multiforme.

Introduction

Glioblastoma multiforme is the most common primary brain tumor, accounting for approximately 60% of all brain tumors. The 5-year survival rate is approximately 5-10% and the median survival is 10 months (Taylor et al., 2019). Treatment of glioblastoma multiforme includes radiotherapy and the use of temozolomide after surgical resection (Salami et al., 2022). It is a highly aggressive cancer with a high invasive ability. For this reason, resistance to treatment may develop or treatment can not be successful (Ghani et al., 2022). Therefore, the identification of new molecular targets that can be effective in glioblastoma multiforme will contribute to the development of new therapeutic strategies.

Sirtuins (SIRTs), are nicotinamide adenine dinucleotide (NAD+) dependent class III histondeacetylases and regulate cellular functions through deacetylation of proteins (Zhang et al., 2020). SIRT2 was the first SIRT identified in *Saccharomyces cerevisiae*. In mammals, there are 7 homologs (SIRT1-SIRT7) of SIRT2 which have a highly conserved central NAD1 binding and a common catalytic domain (Singh et al., 2018). Of these, SIRT1 and SIRT2 are localized in the nucleus and cytoplasm, SIRT1 is predominantly in nucleus and SIRT2 is predominantly in the cytoplasm. SIRT3, SIRT4, and SIRT5 are mitochondrial SIRTs. SIRT6 is found in the nucleus while SIRT7 is found in the nucleolus. The different cellular localization of SIRTs are indicative of their wide range of biological roles such as regulation of cell cycle, cell survival, apoptosis, lipid and glucose homeostasis, metabolism, inflammation, DNA repair, genome stability, and mitochondrial functions (Yamamoto et al., 2007; Shoba et al., 2009; Villalba and Alcaín, 2012;

George and Ahmad, 2016). SIRTs are also associated with various age-related diseases such as metabolic disorders, neurodegenerative disorders, cardiovascular disorders, and cancer (Westphal et al., 2007; Morris, 2012). However, the role of SIRTs in cancer is controversial and complex. It is thought that the efficiency of SIRTs in cancer may be related to various signaling pathways as well as depending on the cancer type (Zhu et al., 2019; Aventaggiato et al., 2021). Therefore, SIRTs, including SIRT2, can be considered both tumor suppressors and tumor promoters. However, the expression of SIRT2, which is expressed in a wide variety of tissues, especially the brain, is higher than the normal tissue in neuroblastoma, uveal melanoma, renal cell carcinoma, and acute myeloid leukemia (Wang et al., 2019; Chen et al., 2020). Moreover, SIRT2 is effective in the proliferation of glioblastoma cells (Funato et al., 2018). Therefore, targeting SIRT2 with various small inhibitors in cancer types, where it is highly expressed or effective during tumorigenesis, may be an important therapeutic approach. Indeed, pharmacological inhibition of SIRT2 has been shown to inhibit the growth of various cancer cells (Cheon et al., 2015; Kozako et al., 2018; Ma et al., 2018).

Therefore, it was aimed to investigate the anti-cancer effect of AK-7, a SIRT2 inhibitor, on U87 human glioblastoma multiforme cells. For this, the effect of AK-7 on proliferation and colony forming capacity of glioblastoma multiforme cells was determined and the apoptotic effect of AK-7 was evaluated with various apoptosis-related assays.

Materials and Methods

Cell culture

The U87 glioblastoma multiforme cell line used in this study was obtained from ATCC. The cells were cultured in high glucose (4.5 g/L) DMEM supplemented with 10%fetal bovine serum (FBS) and 1%penicillin-streptomycin (v/v) at 37°C in a humidified atmosphere containing 5%CO_2. The culture medium was refreshed every 2 days and cells were passaged when confluency reached 80%.

Cell viability

To determine the cytotoxic IC_{50} (the half-maximal inhibitory concentration) dose of AK-7 (Tocris Bioscience) on U87 cell line, firstly, the cells were seeded in a 96-well plate at a density of 2 x 10^3 cells/well and incubated at 37°C for 24 hours. Then, cells were treated with AK-7 at different concentrations (5–250 µM) for 24, 48, and 72 hours. Following treatment, 150 µL of XTT solution was added to each well and incubated at 37°C for 4 hours in the darkness. After the incubation, the absorbance of each sample was measured at a wavelength of 450 nm and 630 nm using a microplate reader (BioTek, Epoch).

Colony formation assay

The colony formation assay was performed to evaluate the effect of 75 and 100 µM doses of AK-7, on colony forming capacity in U87 glioblastoma multiforme cells. U87 cells were seeded in 6-well plates at a density of 2 x 10^3 cells/well. After 24 hours of incubation, 75 and 100 µM doses of AK-7 were treated in triplicate for 48 h. The culture medium was refreshed every other day until colonies were formed. After 8 days of culture, the cells were washed with PBS. Then cells were fixed with 100% methanol at -20°C and stained with 1.0% crystal violet for 10 min. After the cells were photographed under an inverted microscope, each well of the dose and control groups was counted. The average colony numbers of each group were calculated and compared statistically.

Annexin V/7-AAD analysis

To evaluate the apoptotic effect of AK-7 on U87 cells, FITC annexin V apoptosis detection kit with 7-AAD (BioLegend, 640922) was used. FITC annexin V apoptosis detection kit with 7-AAD can detect the rate of necrotic, early apoptotic, and late apoptotic cells in the cell suspension of dose and control group. For this analysis, U87 cells were treated with 75 and 100 µM doses of AK-7 for 48 hours and then washed 2 times with cold BioLegend's cell staining buffer. The cells were resuspended with annexin-V-binding buffer and after the cells were transferred to a flow cytometry tube, 5 µL of FITC annexin V and 5 µL of 7-AAD viability staining solution were added to 100 µL of cell suspension. Finally, the apoptotic effect of AK-7 was measured by flow cytometry using FACSCanto (BD Biosciences).

Cell death detection assay

Cell death detection ELISA^{PLUS} (Roche, 11774425001) assay was used to evaluate the apoptotic effect in U87 glioblastoma multiforme cells treated with two different doses (75 and 100 µM) of AK-7. This assay allows the quantitative detection of DNA fragmentation occurring during apoptosis. For the analysis of this assay, cells were first seeded in 24-well plates at a density of 5 x 10^4 cells/well and then incubated for 24 hours. Afterward, the cells were treated with 75 and 100 µM doses of AK-7 for 48 hours. At the end of 48 hours, cells in each dose group and control group were counted again and seeded in 96-well plates at a density of 10^4 cells/well, and then incubated at 37°C for 4 hours. After the incubation period, the microplate was centrifuged at 200 g for 10 min. After removing the supernatant, each sample was resuspended with 200 µL of lysis buffer and the microplate was incubated for 30 min at room temperature. After the microplate was centrifuged at 200 x g for 10 min, 20 µL of each sample's lysate was transferred to the streptavidin-coated microplate wells, and 80 µL of immunoreagent was added to the

sample wells. After incubation at 300 rpm for 2 hours in a shaker at RT, it was washed 3 times with incubation buffer. 100 µL of ABTS solution was added to each well and incubated for 20 min in a shaker at 250 rpm. After incubation, 100 µL of ABTS stop solution was added and the absorbance values (OD) of each sample were measured in the ELISA reader (BioTek, Epoch) at a wavelength of 405 nm and a reference range of 490 nm.

Caspase-3 activity assay

The effects of AK-7 on caspase-3 activity were performed using caspase-3 assay kit (Biovision, K106) according to the manufacturer's instructions. U87 cells, which were first seeded in 6-well plates at a density of 5 x 10^5 cells/well, were treated with 75 and 100 µM doses of AK-7 for 48 hours, then cells were trypsinized and resuspended with pellet cell lysis buffer and incubated on ice for 10 min. After the cells were centrifuged at 10000 x g for 1 min, the supernatant was transferred to a new tube and the concentration of each sample was measured at 200 µg. After adding 50 µL of 2x reaction buffer (containing 10 mM DTT) and 5 µL of 4 mM DEVD-pNA substrate on each sample, it was incubated at 37°C for 2 hours. The cleaved paranitroanilide with caspase-3 activity in each sample was measured with a microplate reader at 400 nm wavelength (BioTek, Epoch).

Statistical analysis

All experiments were performed in triplicate and all data were presented as mean values ± standard deviation (SD). The differences between groups was

Box 1: qRT-PCR

Principle

Quantitative real time polymerase chain reaction (qRT-PCR) is a method that uses fluorescently labelled probes and dyes, and provides results related to the quantification of nucleic acids by measuring the fluorescent signal that increases simultaneously with amplification. qRT-PCR has a wide range of uses. One of the most common uses is the determination of gene expression at the mRNA level. For this, first of all, total RNA isolation is performed. Then cDNA is synthesized from RNA. Finally, the reaction is performed in a Real Time PCR system using a master mix containing dye that can bind to double-stranded DNA, forward and reverse primers designed according to the target gene sequences and cDNA. The threshold cycle values (Ct) are used for the analysis, corresponding to the cycle in which a significant increase in fluorescence is observed. Normalization is performed with house keeping genes. Differences in gene expression are detected using the 2–ΔΔCT method.

Requirements

cDNA synthesis kit; Chloroform; DNase I enzyme; DNase I enzyme buffer; EDTA; Eppendorf tubes; Ethanol (70%); Isopropanol; Microcentrifuge; Nanodrop (Maestrogen); Nuclease -free dH_2O; PCR tubes; Real-time PCR detection system (Bio-Rad CFX Connect); qPCR MasterMix; 8-Strip PCR tubes; TRIzol reagent; 6-Well plate.

Procedure

Step 1: Total RNA isolation

Media of cells in 6-well plates were removed and 500 µL of TRIzol reagent was added to each well. The homogenate in each well was transferred to eppendorf tubes and incubated for 10 min at room temperature. Then, 200 µL of chloroform was added to each epondorf tube and the tubes were incubated for 15 min at room temperature. At the end of the incubation, centrifugation was performed at 12000 x g for 15 min and the supernatants were transferred to new eppendorf tubes. 500 µL of isopropanol was added to the tubes and incubated for 10 min at room temperature. After incubation, the tubes were centrifuged at 12000 x g for 15 min, then the supernatant was removed and 1 mL of 70%ethanol was added to the pellet. After repeated centrifugation at 7,000 g for 10 min, the supernatant was removed and the pellet was left to dry. After drying, the pellet was dissolved with 30 µL of nuclease-free dH_2O. In order to determine the quantity and quality of the isolated RNAs, 1 µL of each RNA sample was taken and measurements were made in a nanodrop (Maestrogen). RNA samples with UV measurements between 2 ± 0.1 for A_{260}/A_{280} and 2.0-2.4 for A_{260}/A_{230} were used in the analyses.

Step 2: Treatment with DNase I

In order to eliminate possible genomic DNA contamination, RNA samples were treated with DNAse-I enzyme before cDNA synthesis. For this purpose, 2 µL of 1U/µL DNAse-I enzyme and 2 µL of 10x reaction buffer were added to 2 µg RNA sample and the total volume was made up to 18 µL with nuclease-free dH_2O. After incubation at 37°C for 30 min, 2 µL of 50 mM EDTA was added to the samples and the reaction was stopped by incubation at 65°C for 10 min.

Step 3: cDNA synthesis

For cDNA synthesis, 4 µL of the reaction mixture included in the kit and 1 µL of Reverse Transcriptase enzyme were added to 1 µg total RNA, and the volume of the mixture was made up to 20 µL with nuclease-free water. Then, cDNA synthesis protocol was applied as 5 min at 25°C, 20 min at 46°C and 1 min at 95°C.

Step 4: qRT-PCR

qRT-PCR analysis was performed using qPCR mastermix (BrightGreen 2x qPCR MasterMix – ROX, ABM, MasterMix-R), which can bind to double-stranded DNA. For this purpose, reaction mixtures containing 5 µL BrightGreen 2X qPCR MasterMix, 5 pMol forward primer, 5 pMol reverse primer and 2 µL cDNA were prepared. The reaction was carried out in a Real-time PCR System (Bio-Rad, CFX Connect) in 40 cycles using the PCR protocol consisting of 10 min at 95°C, 15 sec at 95°C and 60 sec at 60°C. Ct values of each reaction were used for the analysis. *GAPDH* and *ACTB* was used as a reference gene for normalization and $2^{-\Delta\Delta CT}$ was used to analyze the relative changes in gene expressions.

References

Çınar et al., 2021a; Çınar et al., 2021b; Güçlü et al., 2021

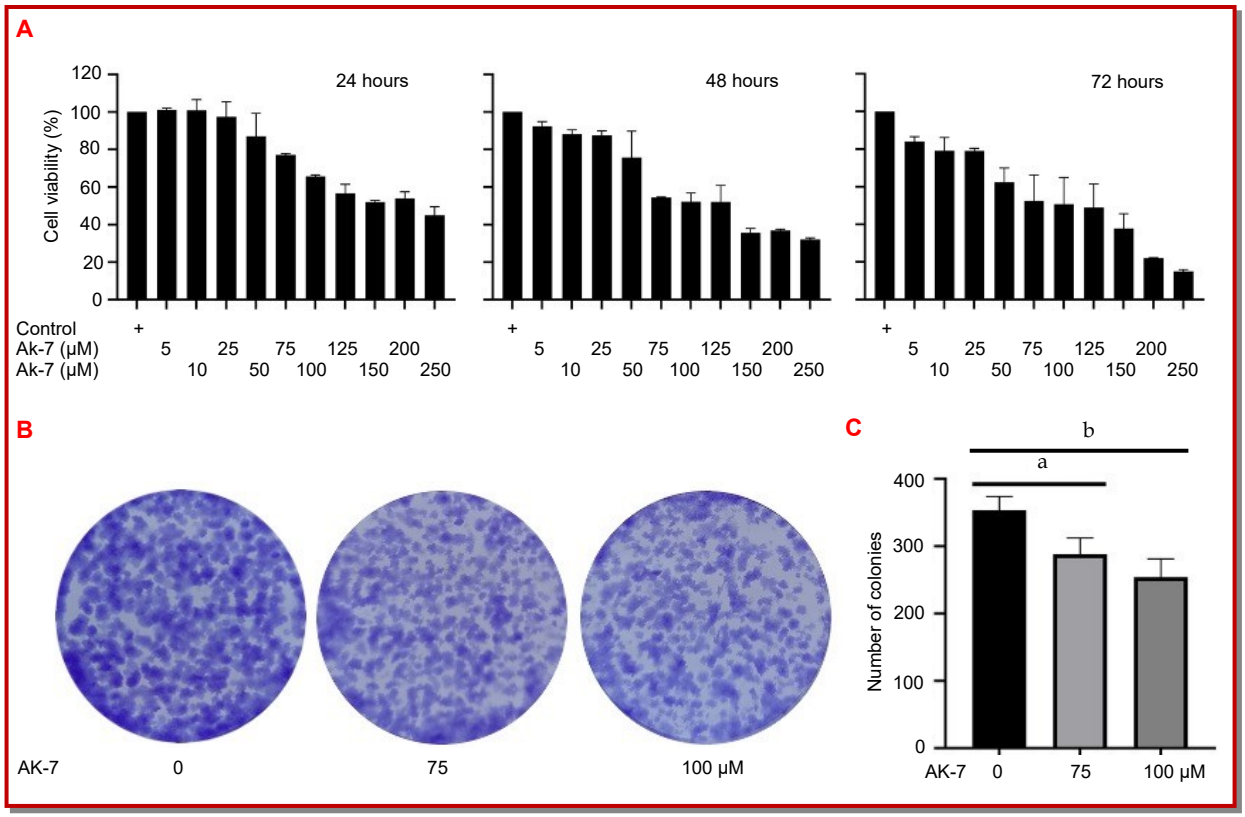

Figure 1: AK-7 reduced the survival and colony formation of glioblastoma multiforme cells. Dose- (5, 10, 25, 50, 75, 100, 125, 150, 200, and 250 μM) and time- (24, 48, 72 hours) dependent effect of AK-7 on the U87 human glioblastoma multiforme cell line (A). Colony formation assay was performed to analyze the colony forming capacity of U87 cells which were treated with different concentrations (75 and 100 μM) of AK-7 ($^{a}p<0.05$; $^{b}p<0.01$) (B-C)

evaluated with Student's t test and one-way ANOVA. IC_{50} value was calculated using GraphPad Prism 8.0.2 version. Also, all statistical analysis and bar graphs were performed with GraphPad Prism 8.0.2 version. RT2 Profiler™ PCR array data analysis program was used for statistical determination of changes in mRNA expression level. $p<0.05$ value was considered statistically significant.

Results

U87 glioblastoma multiforme cell proliferation and colony formation

XTT cell viability assay was used to determine whether AK-7 affects U87 cell proliferation. U87 cells were exposed to various concentrations of AK-7. It was determined that AK-7 inhibited cell proliferation in a dose- and time-dependent manner (Figure 1A). The IC_{50} value of AK-7 induced inhibition at various concentrations at 48 hours was identified as 107.0 μM in U87 cell. The effects of 75 and 100 μM doses of AK-7 on the colony forming capacity on U87 cells were evaluated according to control group (untreated cells with AK-7). Similarly, it was found that colony formation significantly decreased by treatment 75 and 100 μM doses of AK-7 comparison to the control group on U87 cells. However, there was no significant difference in colony formation ability between 75 and 100 μM dose groups (Figure 1BC).

Apoptosis of U87 glioblastoma multiforme cells

To evaluate whether the inhibition mechanism of AK-7 on the U87 glioblastoma multiforme cells is apoptosis-mediated, we first performed the FITC-annexin V/7-AAD analysis. For this analysis, U87 cells were treated with 75 and 100 μM doses of AK-7 for 48 hours. Compared to the control group, it was determined that cellular apoptosis (early and late apoptosis) rate was significantly increased in cells treated with AK-7 in a dose-dependent manner. Also, a significant increase was observed in the apoptosis rate between dose groups of AK-7 (Figure 2A-B) ($p<0.05$). The degree of apoptosis was shown as the enrichment factor calculated as follows at bar graph: Enrichment factor = DNA fragments in the 75 and 100 μM AK-7 treated sample / DNA fragments in the control. According to the results of this analysis, it was found that AK-7 caused a significant increase in the enrichment factor in a dose-dependent manner when compared to the control group. In addition, a similarly significant difference was also determined between the groups treated with 75 and 100 μM doses of AK-7 (Figure 2C) ($p<0.05$). It

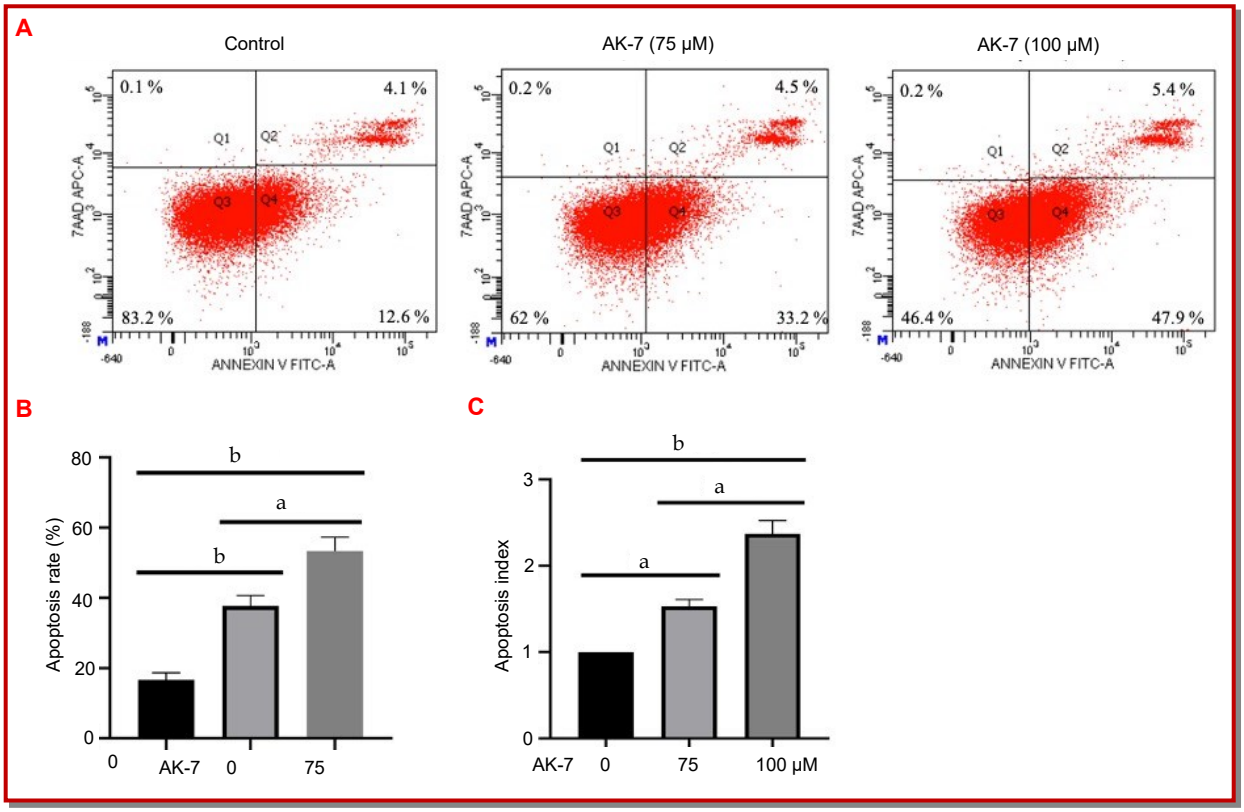

Figure 2: AK-7 promoted apoptosis of U87 glioblastoma multiforme cells. U87 cells were treated with two different concentrations (75 and 100 µM) of AK-7 for 48 hours. After treatment, annexin V/7-AAD analysis was performed to determine the necrotic, early and late apoptotic cells in each group (A-B). Apoptotic cell death due to DNA fragmentation was evaluated using a cell death detection ELISA^{PLUS} kit ($^{a}p<0.01$, $^{b}p<0.001$) (C)

was demonstrated that AK-7 induced DNA fragmentation.

Apoptosis of U87 glioblastoma multiforme cells through the caspase pathway

To investigate the molecular mechanism of AK-7 inducing apoptosis of U87 glioblastoma multiforme cells, mRNA expression levels of cell apoptosis-related genes were determined by qRT-PCR. Analysis of mRNA expression levels of genes after treatment of 75 and 100 µM doses of AK-7 was compared with control group cells and the differences between groups were shown in Figure 3A. The mRNA expression levels of *CASP7*, *CASP8*, *CASP10*, *CYCS*, *PPARG*, *FAS*, *FADD* increased in cells treated with both dose groups of AK-7. Additionally, it was found that *CASP9*, *TNF*, *TNFR1* and *TNFR2* mRNA expression levels increased significantly only in cells treated with 100 µM AK-7 dose group. According to the results of caspase-3 activity test, the fold change of 75 and 100 µM dose groups of AK-7 increased significantly compared to the control group, and there was also a significant difference between the 75 and 100 µM dose groups of AK-7 (Figure 3B) ($p<0.05$).

Discussion

Targeting various molecules that play a role in tumor development is one of the important therapeutic approaches to cancer. One of these molecular targets is SIRTs, known as NAD+ dependent class III histondeacetylases. SIRT2, which is in the SIRT family, is associated with various physiological and pathological processes and has a controversial role as a tumor suppressor or tumor promoter in cancer (Roshdy et al., 2021).

The tumor suppressive property of SIRT2 is associated with maintaining genome integrity and regulating the anaphase-promoting complex/cyclosome activity. Furthermore, SIRT2 deficiency in mice has been shown to cause genetic instability and tumorigenesis (Kim et al., 2011). SIRT2 negatively regulates the expression of JMJD2A, which is associated with poor survival in non–small cell lung cancer (NSCLC), and inhibits proliferation, colony formation, and tumor growth of NSCLC cells (Xu et al., 2015). In colorectal cancer cells, SIRT2 is one of the targets of Wnt/β-catenin signaling and has a tumor suppressor role by enabling the differentiation of colorectal cancer cells (Li et al., 2021). The lack of

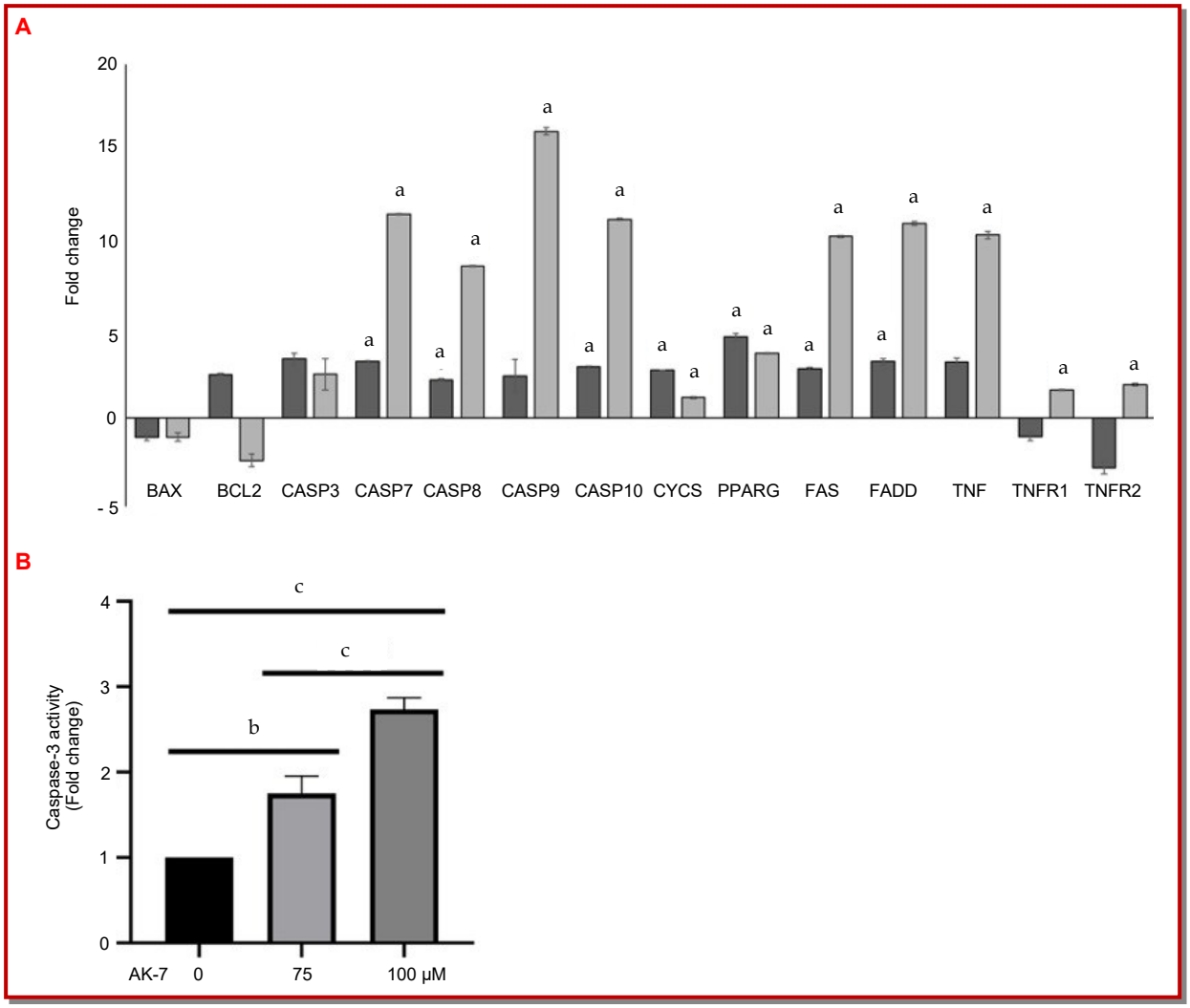

Figure 3: Effect of AK-7 on caspase pathway mediated apoptosis in U87 GBM cells. After treatment with AK-7 (75 and 100 µM) for 48 hours, mRNA expression levels of apoptosis-associated genes were analyzed by qRT-PCR (A). The effects of two different concentrations of AK-7 compared to the control group on caspase-3 activity were performed using the caspase-3 assay kit ($^{a}p<0.05$, $^{b}p<0.01$, $^{c}p<0.001$) (B)

suppression of cyclin-dependent kinase 4 due to the decrease in SIRT2 expression increases the proliferation of ovarian cancer cells (Du et al., 2017). In addition, SIRT2 overexpression increases the cisplatin sensitivity of cisplatin-resistant ovarian cancer cells (Wang et al., 2020).

SIRT2 can also contribute to the duration of tumorigenesis by various mechanisms. In a study with glioblastoma cells, SIRT2 regulates the transcriptional activity of p73 and contributes to the proliferation of glioma stem cells and glioma cells (Funato et al., 2018). SIRT2 induces epithelial-mesenchymal transition through the glycogen synthase kinase-3β/β-catenin pathway in hepatocellular carcinoma (HCC), and downregulation of SIRT2 reduces migration and invasion in HCC cells (Chen et al., 2013; Huang et al., 2017). Hu et al. (2018) reported that SIRT2 expression is high in colorectal cancer tissues, and silencing of SIRT2 suppresses tumor angiogenesis through STAT3/VEGFA inactivation. Similarly, SIRT2 expression is high in patients with relapsing acute myeloid leukemia, and silencing of SIRT2 in drug-resistant HL60/A cells decreases MRP1 levels, increases drug accumulation, and stimulates apoptosis (Xu et al., 2016).

Although the tumor suppressive property of SIRT2 is mentioned, SIRT2 inhibitors can cause anti-cancer effects in various studies targeting SIRT2 pharmacologically. AGK2, a SIRT2 inhibitor, arrests the cell cycle and inhibits cell growth in cervical cancer cells with high SIRT2 expression (Singh et al., 2015). TM, a selective SIRT2 inhibitor, exerts an anti-cancer effect through the degradation of c-Myc in breast cancer cells (Jing et al., 2016). Various SIRT1/2 inhibitors induce p53 acetylation and stimulate cell death in breast cancer cells (Peck

et al., 2010). AK-1 induces proteasomal degradation of transcription factor Snail and thus arrests the cell cycle in colon cancer cells (Cheon et al., 2015).

In this study, it was aimed to investigate the possible anti-cancer effect of AK-7 in glioblastoma multiforme cells. Although it is known that AK-7 inhibits neurodegenerative processes and has a neuroprotective effect, there is no information about the anti-cancer activity of AK-7 (Chopra et al., 2012; Chen et al., 2015; Biella et al., 2016). To investigate the possible anti-cancer effect of AK-7 in glioblastoma multiforme cells, we first performed cytotoxicity analysis. According to the cytotoxicity analysis results, AK-7 inhibited cell proliferation in glioblastoma multiforme cells in a dose- and time-dependent manner. The IC_{50} dose of AK-7 in U87 cells was found to be 107.0 µM for 48 hours. In subsequent analyzes, U87 cells were treated with 75 µM and 100 µM AK-7 for 48 hours to reveal whether there was a dose-dependent effect of AK-7. The effect of AK-7 on cell proliferation was also evaluated by colony formation analysis and it was observed that treatment with 75 µM and 100 µM AK-7 inhibited the colony forming capacity of U87 cells.

In this study, the possible anti-cancer activity of AK-7 in glioblastoma multiforme cells was evaluated with various analyzes to determine apoptosis. According to Annexin V analysis results, treatment with 75 µM and 100 µM AK-7 significantly increased the %apoptosis rate in glioblastoma multiforme cells compared to the control group. In addition, the apoptosis-inducing effect of AK-7 increased in a dose-dependent manner.

Apoptosis is characterized by a series of typical morphological changes such as shrinkage of cell and nucleus, chromatin condensation, and formation of apoptotic bodies. At this stage, fragmentation of chromosomal DNA into oligonucleosome-sized fragments is also one of the important markers of apoptosis (Elmore, 2007; Zhang and Xu, 2000). According to DNA fragmentation analysis results, DNA fragmentation was induced in U87 cells after treatment with 75 and 100 µM AK-7. It was also observed that DNA fragmentation increased depending on the dose of AK-7.

Caspases are at the center of the apoptosis mechanism in the cell, and apoptosis occurs in two pathways, in which a large number of molecules are involved: the extrinsic pathway and the intrinsic pathway. The extrinsic pathway is initiated by the interaction of various death receptors with their ligands. Then, the death-inducing signaling complex (DISC) is formed with adapter proteins such as TNF receptor-associated death domain (TRADD) and Fas-associated death domain (FADD), procaspases-8 and -10. This formation causes activation of caspase-8 and 10, and then apoptosis is induced by activation of caspase-3, -6 and -7 (Ashkenazi, 2008; Wong, 2011).

In the intrinsic pathway, Bcl-2 family, which consists of proapoptotic and antiapoptotic members, is involved and especially the balance between Bcl-2 and Bax is determinant in the release of cytochrome c from mitochondria to the cytoplasm. Cytochrome c released into the cytoplasm interacts with Apaf-1 and caspase-9 is activated. And, apoptosis is induced by the activation of caspase-3 by active caspase-9 (Elmore, 2007; Inoue et al., 2009). In this study, the anti-cancer effect of AK-7 was evaluated at the molecular level by analyzing the expression levels of genes associated with extrinsic and intrinsic pathways of apoptosis. For this purpose, expression levels of *CASP8*, *CASP10*, *FAS*, *FADD*, *TNF*, *TNFR1* and *TNFR2* genes associated with the extrinsic pathway; *BAX*, *BCL2*, *CASP7*, *CYCS* and *PPARG* genes associated with the intrinsic pathway, and *CASP3* gene associated with both pathways were determined in qRT -PCR analysis after treatment with AK-7. According to qRT-PCR results, AK-7 significantly increased the expression of both extrinsic and intrinsic pathway-related genes in glioblastoma multiforme cells. As mentioned above, caspase-3 acts as an effector caspase and plays a central role in both extrinsic and intrinsic pathways of apoptosis. Therefore, active caspase-3 activity in cells is directly related to apoptosis. In this study, active caspase-3 activity was also evaluated, and a significant increase in caspase-3 activity was detected after treatment with 75 µM and 100 µM AK-7 when compared with the control group. In addition, it was determined that caspase-3 activity increased depending on the dose of AK-7.

Conclusion

AK-7, a selective SIRT2 inhibitor, suppresses cell proliferation and induces apoptosis in a dose-dependent manner in glioblastoma multiforme cells. These findings suggest that SIRT2 may be a therapeutic target in glioblastoma multiforme.

Financial Support

Self-funded

Conflict of Interest

Authors declare no conflict of interest

References

Ashkenazi A. Targeting the extrinsic apoptosis pathway in cancer. Cytokine Growth Factor Rev. 2008; 19: 325-31.

Aventaggiato M, Vernucci E, Barreca F, Russo MA, Tafani M. Sirtuins' control of autophagy and mitophagy in cancer.

Pharmacol Ther. 2021; 221: 107748.

Biella G, Fusco F, Nardo E, Bernocchi O, Colombo A, Lichtenthaler SF, Forloni G, Albani D. Sirtuin 2 inhibition improves cognitive performance and acts on amyloid-β protein precursor processing in two Alzheimer's disease mouse models. J Alzheimer's Dis. 2016; 53: 1193-207.

Chen G, Huang P, Hu C. The role of SIRT2 in cancer: A novel therapeutic target. Int J Cancer. 2020; 147: 3297-304.

Chen J, Chan AW, To KF, Chen W, Zhang Z, Ren J, Song C, Cheung YS, Lai PB, Cheng SH, Ng MH, Huang A, Ko BC. SIRT2 overexpression in hepatocellular carcinoma mediates epithelial to mesenchymal transition by protein kinase B/glycogen synthase kinase-3β/β-catenin signaling. Hepatology. 2013; 57: 2287-98.

Chen X, Wales P, Quinti L, Zuo F, Moniot S, Herisson F, Rauf NA, Wang H, Silverman RB, Ayata C, Maxwell MM, Steegborn C, Schwarzschild MA, Outeiro TF, Kazantsev AG. The sirtuin-2 inhibitor AK7 is neuroprotective in models of Parkinson's disease but not amyotrophic lateral sclerosis and cerebral ischemia. PLoS One. 2015; 10: e0116919.

Cheon MG, Kim W, Choi M, Kim JE. AK-1, a specific SIRT2 inhibitor, induces cell cycle arrest by downregulating Snail in HCT116 human colon carcinoma cells. Cancer Lett. 2015; 356: 637-45.

Chopra V, Quinti L, Kim J, Vollor L, Narayanan KL, Edgerly C, Cipicchio PM, Lauver MA, Choi SH, Silverman RB, Ferrante RJ, Hersch S, Kazantsev AG. The sirtuin 2 inhibitor AK7 is neuroprotective in Huntington's disease mouse models. Cell Rep. 2012; 2: 1492-97.

Çınar Ayan İ, Çetinkaya S, Dursun HG, Süntar İ. Bioactive compounds of Rheum ribes L. and its anticancerogenic effect via induction of apoptosis and miR-200 family expression in human colorectal cancer cells. Nutr Cancer. 2021a; 73: 1228-43.

Çınar Aİ, Güçlü E, Dursun H.G, Vural H. Tomentosin shows anticancer effect on U87 human glioblastoma multiforme cells. Bull Biotechnol. 2021b; 2: 23-26.

Du Y, Wu J, Zhang H, Li S, Sun H. Reduced expression of SIRT2 in serous ovarian carcinoma promotes cell proliferation through disinhibition of CDK4 expression. Mol Med Rep. 2017; 15: 1638-46.

Elmore S. Apoptosis: A review of programmed cell death. Toxicol Pathol. 2007; 35: 495-516.

Funato K, Hayashi T, Echizen K, Negishi L, Shimizu N, Koyama-Nasu R, Nasu-Nishimura Y, Morishita Y, Tabar V, Todo T, Ino Y, Mukasa A, Saito N, Akiyama T. SIRT2-mediated inactivation of p73 is required for glioblastoma tumorigenicity. EMBO Rep. 2018; 19: e45587.

George J, Ahmad N. Mitochondrial sirtuins in cancer: Emerging roles and therapeutic potential. Cancer Res. 2016; 76: 2500-06.

Ghani ARI, Yahya EB, Allaq AA, Khalil ASA. Novel insights into genetic approaches in glioblastoma multiforme therapy. Biomed Res Ther. 2022; 9: 4851-64.

Güçlü E, Eroğlu Güneş C, Kurar E, Vural H. Knockdown of lncRNA HIF1A-AS2 increases drug sensitivity of SCLC cells in association with autophagy. Med Oncol. 2021; 38: 113.

Hu F, Sun X, Li G, Wu Q, Chen Y, Yang X, Luo X, Hu J, Wang G. Inhibition of SIRT2 limits tumour angiogenesis via inactivation of the STAT3/VEGFA signalling pathway. Cell Death Dis. 2018; 10: 9.

Huang S, Zhao Z, Tang D, Zhou Q, Li Y, Zhou L, Yin Y, Wang Y, Pan Y, Dorfman RG, Ling T, Zhang M. Down-regulation of SIRT2 inhibits invasion of hepatocellular carcinoma by inhibiting energy metabolism. Transl Oncol. 2017; 10: 917-27.

Inoue S, Browne G, Melino G, Cohen GM. Ordering of caspases in cells undergoing apoptosis by the intrinsic pathway. Cell Death Differ. 2009; 16: 1053-61.

Jing H, Hu J, He B, Negrón Abril YL, Stupinski J, Weiser K, Carbonaro M, Chiang YL, Southard T, Giannakakou P, Weiss RS, Lin H. A SIRT2-Selective inhibitor promotes c-Myc oncoprotein degradation and exhibits broad anticancer activity. Cancer Cell. 2016; 29: 297-310.

Kim HS, Vassilopoulos A, Wang RH, Lahusen T, Xiao Z, Xu X, Li C, Veenstra TD, Li B, Yu H, Ji J, Wang XW, Park SH, Cha YI, Gius D, Deng CX. SIRT2 maintains genome integrity and suppresses tumorigenesis through regulating APC/C activity. Cancer Cell. 2011; 20: 487-99.

Kozako T, Mellini P, Ohsugi T, Aikawa A, Uchida YI, Honda SI, Suzuki T. Novel small molecule SIRT2 inhibitors induce cell death in leukemic cell lines. BMC Cancer. 2018; 18: 791.

Li C, Zhou Y, Kim JT, Sengoku T, Alstott MC, Weiss HL, Wang Q, Evers BM. Regulation of SIRT2 by Wnt/β-catenin signaling pathway in colorectal cancer cells. Biochim Biophys Acta Mol Cell Res. 2021; 1868: 118966.

Ma W, Zhao X, Wang K, Liu J, Huang G. Dichloroacetic acid (DCA) synergizes with the SIRT2 inhibitor sirtinol and AGK2 to enhance anti-tumor efficacy in non-small cell lung cancer. Cancer Biol Ther. 2018; 19: 835-46.

Morris BJ. Seven sirtuins for seven deadly diseases of aging. Free Radic Biol Med. 2013; 56: 133-71.

Peck B, Chen CY, Ho KK, Di Fruscia P, Myatt SS, Coombes RC, Fuchter MJ, Hsiao CD, Lam EW. SIRT inhibitors induce cell death and p53 acetylation through targeting both SIRT1 and SIRT2. Mol Cancer Ther. 2010; 9: 844-55.

Roshdy E, Mustafa M, Shaltout AE, Radwan MO, Ibrahim MAA, Soliman ME, Fujita M, Otsuka M, Ali TFS. Selective SIRT2 inhibitors as promising anti-cancer therapeutics: An update from 2016 to 2020. Eur J Med Chem. 2021; 224: 113709.

Salami R, Salami M, Mafi A, Vakili O, Asemi Z. Circular RNAs and glioblastoma multiforme: Focus on molecular mechanisms. Cell Commun Signal. 2022; 20: 13.

Shoba B, Lwin ZM, Ling LS, Bay BH, Yip GW, Kumar SD. Function of sirtuins in biological tissues. Anat Rec (Hoboken). 2009; 292: 536-43.

Singh CK, Chhabra G, Ndiaye MA, Garcia-Peterson LM, Mack NJ, Ahmad N. The role of sirtuins in antioxidant and redox signaling. Antioxid Redox Signal. 2018; 28: 643-61.

Singh S, Kumar PU, Thakur S, Kiran S, Sen B, Sharma S, Rao

VV, Poongothai AR, Ramakrishna G. Expression/localization patterns of sirtuins (SIRT1, SIRT2, and SIRT7) during progression of cervical cancer and effects of sirtuin inhibitors on growth of cervical cancer cells. Tumour Biol. 2015; 36: 6159-71.

Taylor OG, Brzozowski JS, Skelding KA. Glioblastoma multiforme: An overview of emerging therapeutic targets. Front Oncol. 2019; 9: 963.

Villalba JM, Alcaín FJ. Sirtuin activators and inhibitors. Biofactors 2012; 38: 349-59.

Wang W, Im J, Kim S, Jang S, Han Y, Yang KM, Kim SJ, Dhanasekaran DN, Song YS. ROS-induced SIRT2 Up-regulation contributes to cisplatin sensitivity in ovarian cancer. Antioxidants (Basel) 2020; 9: 1137.

Wang Y, Yang J, Hong T, Chen X, Cui L. SIRT2: Controversy and multiple roles in disease and physiology. Ageing Res Rev. 2019; 55: 100961.

Westphal CH, Dipp MA, Guarente L. A therapeutic role for sirtuins in diseases of aging? Trends Biochem Sci. 2007; 32: 555-60.

Wong RS. Apoptosis in cancer: From pathogenesis to treatment. J Exp Clin Cancer Res. 2011; 30: 87.

Xu H, Li Y, Chen L, Wang C, Wang Q, Zhang H, Lin Y, Li Q, Pang T. SIRT2 mediates multidrug resistance in acute myelogenous leukemia cells via ERK1/2 signaling pathway. Int J Oncol. 2016; 48: 613-23.

Xu W, Jiang K, Shen M, Qian Y, Peng Y. SIRT2 suppresses non-small cell lung cancer growth by targeting JMJD2A. Biol Chem. 2015; 396: 929-36.

Yamamoto H, Schoonjans K, Auwerx J. Sirtuin functions in health and disease. Mol Endocrinol. 2007; 21: 1745-55.

Zhang GZ, Deng YJ, Xie QQ, Ren EH, Ma ZJ, He XG, Gao YC, Kang XW. Sirtuins and intervertebral disc degeneration: Roles in inflammation, oxidative stress, and mitochondrial function. Clin Chim Acta. 2020; 508: 33-42.

Zhang JH, Xu M. DNA fragmentation in apoptosis. Cell Res. 2000; 10: 205-11.

Zhu S, Dong Z, Ke X, Hou J, Zhao E, Zhang K, Wang F, Yang L, Xiang Z, Cui H. The roles of sirtuins family in cell metabolism during tumor development. Semin Cancer Biol. 2019; 57: 59-71.

Author Info
Ebru Güçlü (Principal contact)
e-mail: ebruavc.87@gmail.com